Adsorption of acetone molecules on proton ordered ice. A molecular dynamics study

S. Picaud and P. N. M. Hoang

Citation: The Journal of Chemical Physics **112**, 9898 (2000); doi: 10.1063/1.481627
View online: http://dx.doi.org/10.1063/1.481627
View Table of Contents: http://scitation.aip.org/content/aip/journal/jcp/112/22?ver=pdfcov
Published by the AIP Publishing

Adsorption of acetone molecules on proton ordered ice. A molecular dynamics study

S. Picaud[a] and P. N. M. Hoang
Laboratoire de Physique Moléculaire—UMR CNRS 6624, Faculté des Sciences, La Bouloie, Université de Franche-Comté, 25030 Besançon Cedex, France

(Received 6 December 1999; accepted 16 March 2000)

The adsorption of acetone molecules on a proton ordered ice Ih(0001) surface was studied using classical molecular dynamics simulations between 50 and 150 K. At low coverage, we show that acetone molecules form an ordered monolayer on this ice surface, which is stable for $T \leqslant 100$ K. At higher temperature, it exhibits orientational disordering, though local translational order remains. Preliminary simulations at higher coverage indicates the formation of additional ordered layers above the first monolayer, which are also stable below 100 K. These results support previous conclusions on the acetone/ice interactions based on the interpretation of experimental data.
 [S0021-9606(00)71022-1]

I. INTRODUCTION

The characterization of the interactions between small molecules and ice particles has been an active field of research for several years.[1] Until now, careful attention has been paid to the adsorption of halogenated molecules due to the role played by the chlorofluorocarbons (CFCs) in the ozone depletion.[2] Indeed, it is now accepted that ice particles contained in polar stratospheric clouds (PSCs) catalyze reactions, converting inert halogenated species into photoactive dichlorine and difluorine molecules.[3] Although the overall chemistry occurring on PSCs is quite well understood at the macroscopic level, the molecular mechanisms involved in these reactions are still unclear. Moreover, from a more fundamental point of view, the surface chemistry of molecular solids such as ice is not as well understood as the surface reactivity of metals or ionic crystals.

Small organic molecules are generally characterized by large electric moments which can interact strongly with the electric field created at the surface of ice particles.[4] At short distances, they can also form hydrogen bonds with water molecules. As a consequence, such small organic molecules are good candidates for the study of the influence of the ice structure and dynamics on the adsorption properties of atmospheric gases.

This is the case of the acetone molecule which is relatively abundant in the troposphere, where its photodissociation leads to the formation of HO_x radicals, especially at high altitude where other sources of HO_x are not present.[5,6] An increase of the concentration of HO_x in the troposphere can increase the ozone production.[7] Moreover, these radicals react with NO_2 and SO_2 to form nitric and sulfuric acids which strongly influence the formation and composition of aerosols and the formation of condensation nuclei for the PSCs.[8] Furthermore, from an experimental point of view, the physico–chemical properties of the acetone molecule allow much easier adsorption measurements than molecules such as HCl or HNO_3, for example.[9] Nevertheless, very few experiments have been conducted on the interaction between acetone and ice surfaces. As far as we know, only the work by Schaff and Roberts[10,11] has been published on this system. These authors have studied the adsorption properties of acetone at different exposures, on annealed and unannealed ice films (H_2O and D_2O) deposited on W(100) and Pt(111) by thermal desorption spectroscopy (TDS) between 100 and 180 K, and under ultrahigh vacuum conditions. They showed that an unannealed ice film corresponds to an amorphous structure which transforms into a crystalline structure after annealing. Two states, labeled as α- and β-acetone, respectively, were observed from the unannealed surface at 140 and 157 K, while only the lower temperature α state was observed from annealed ice. However, note that, at very low exposures, the two states are also observed on annealed ice. The activation energies for α- and β desorption are approximately 35 and 40 kJ/mol, respectively. From these experiments, it was concluded that acetone is entirely molecularly adsorbed and that β acetone is connected to a hydrogen-bonded state, while α acetone is physisorbed.[10] Moreover, infrared spectroscopy measurements[11] have shown that vibrational frequencies of adsorbed acetone are close to those of condensed acetone, except for the carbonyl stretch mode, for which two bands that grow in at different acetone exposures are observed on both amorphous and crystalline ice. The low frequency peak at 1703 cm^{-1}, which grows in first, is redshifted by 14 cm^{-1} when compared to the bulk value. This peak was attributed to acetone hydrogen bonded to water, on the basis of the calculated value for the carbonyl stretch mode in the acetone–water dimer (1702.7 cm^{-1}).[12] The higher frequency peak at 1717 cm^{-1}, which grows in after the previous first peak is nearly saturated, was related to either bulk or physisorbed acetone. Furthermore, adsorption of acetone on ice resulted rapidly in the complete disappearance of the free O–D stretch on both annealed and unannealed surfaces, a feature which is consistent with the formation of hydrogen bonds to the carbonyl oxygens.

[a]Electronic mail: sylvain.picaud@univ-fcomte.fr

These experiments have shown that acetone presents a rich and varied surface chemistry on ice which is not fully understood. Therefore, we use numerical methods to investigate the adsorption of such a molecule on a hexagonal ice Ih(0001) surface. At finite temperature it seems that a realistic ice surface could be a proton disordered model in which the arrangement of the H atoms is quasirandom within the constraints of the ice rules.[13,14] Although such proton disordered ice crystals are available in the literature,[15–17] it should be pointed out that their stability in the simulations strongly depends on the potential used for the interaction between water molecules. For example, it has been recently shown that when the TIP4P model,[18] which is well known to give results in fair agreement with many experimental data,[19] is used for characterizing the interaction between water molecules, a proton ordered hexagonal ice is the most stable structure at 1 atm when compared to various proton disordered ice crystals.[20] Moreover, since many different proton disordered structures can be generated, a statistical study on various surfaces would be required in order to investigate the influence of the proton disorder on the adsorption of polar molecules such as acetone.

In the present paper, we have chosen to simulate the adsorption of acetone on a proton ordered hexagonal ice crystal. Indeed, previous study by optimization of classical potentials[21] has shown that a perfectly ordered monolayer of acetone molecules can be formed at the surface of such proton ordered ice crystal at 0 K. Here, on the basis of the same potentials, we perform classical molecular dynamics (MD) simulations in order to investigate the structure and the dynamics of this acetone layer between 50 and 150 K. We also discuss preliminary results on the influence of the acetone coverage on the adsorbed layer.

In Sec. II, the details of the molecular dynamics simulation are given, and the corresponding results are presented in Sec. III. These results are discussed and compared with available experimental data in Sec. IV.

II. MOLECULAR DYNAMICS CALCULATIONS

A. Interaction potential

The intermolecular potentials used in the present study consist of site–site potentials $V(r_{ij})$ which contain Coulombic and Lennard-Jones contributions. These potentials are written as

$$V(r_{ij})=\frac{M_i^{(0)}M_j^{(0)}}{r_{ij}}+4\epsilon_{ij}\left[\left(\frac{\sigma_{ij}}{r_{ij}}\right)^{12}-\left(\frac{\sigma_{ij}}{r_{ij}}\right)^{6}\right], \tag{1}$$

where r_{ij} is the distance between the ith and jth sites of the interacting molecules, $M_i^{(0)}$ is a point charge located at the ith site, and ϵ,σ are the usual Lennard-Jones parameters. For the interaction V_{aa} between the acetone molecules, we use the four-sites model proposed by Ferrario *et al.*[22] in which charges and dispersion–repulsion centers are located on the C and O atoms. Note that the methyl group is treated as one site centered on the carbon atom. The TIP4P model is used for water[18] (V_{ww} potential) since it is well known that this model can accurately reproduce structures and dynamics properties of both real ice and water.[19] The interaction V_{aw} between water and acetone is defined in the same way, where the cross interactions are obtained by using the usual Lorentz–Berthelot combining rules. The various potential parameters are summarized in Table I. Note that here, we used a nonpolarizable model for both water and acetone, since simulations with such polarizable models are much more time consuming.[23] It has been shown in a recent Monte Carlo simulation of polarizable liquid acetone that the induced polarization affects the energy and dielectric properties, but not the structural properties.[24] In the simulation, all interactions between sites are damped through a switching function $S(R)$. So, the effective interactions between two molecules are obtained by multiplying the pair interactions with $S(R)$. This function $S(R)$, where R is the centers of mass separation between molecules, is defined as[25]

$$\begin{aligned} S(R)&=1 \quad R<11.0 \text{ Å},\\ S(R)&=0 \quad R>11.5 \text{ Å},\\ S(R)&=1-\alpha^3(10-15\alpha+6\alpha^2) \quad 11.0\leqslant R\leqslant 11.5 \text{ Å},\\ \alpha&=2(R-11.0). \end{aligned} \tag{2}$$

At the boundaries of the switching region, the potential energy is continuous and the switching function first and second derivatives are zero.

TABLE I. Parameters for the various potentials used in the present study. The coordinates of the different sites are given with respect to the molecular frame located at the center of mass.

Site	Coordinates (Å)	$M^{(0)}$ (e)	ϵ (meV)	σ (Å)
Water[a]				
O	$(x,y,z)=(0.0;0.0;-0.065)$	0.00	6.732	3.152
H	$(x,y,z)=(0.757;0.0;0.521)$	0.52	–	–
H	$(x,y,z)=(-0.757;0.0;0.521)$	0.52	–	–
m[b]	$(x,y,z)=(0.0;0.0;0.085)$	−1.04	–	–
Acetone[c]				
O	$(x,y,z)=(0.0;0.0;-1.320)$	−0.502	9.118	2.960
C_O	$(x,y,z)=(0.0;0.0;-0.104)$	0.566	4.559	3.750
C	$(x,y,z)=(-1.272;0.0;0.700)$	−0.032	7.334	3.880
C	$(x,y,z)=(1.272;0.0;0.700)$	−0.032	7.334	3.880
H	$(x,y,z)=(-2.173;0.0;0.074)$	–	–	–
H	$(x,y,z)=(-1.363;-0.876;1.356)$	–	–	–
H	$(x,y,z)=(-1.363;0.876;1.356)$	–	–	–
H	$(x,y,z)=(2.173;0.0;0.074)$	–	–	–
H	$(x,y,z)=(1.363;-0.876;1.356)$	–	–	–
H	$(x,y,z)=(1.363;0.876;1.356)$	–	---	–

[a]Reference 18.
[b]Additional electric site.
[c]Reference 22.

B. Details of the simulation

We consider adsorption on the (0001) basal plane of a proton ordered hexagonal ice crystal. The size of the simulation box is defined from an orthorhombic unit cell of dimensions $L_x=8.98$ Å, $L_y=7.78$ Å, $L_z=7.33$ Å.[26] This simulation box contains four bilayers of moving water molecules which form a slab 14.66 Å thick. These moving water molecules are placed on a slab consisting of two bilayers of fixed

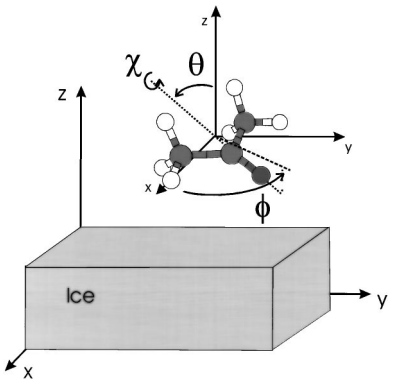

FIG. 1. Geometry of the adsorbed molecule. The acetone orientation (ϕ,θ,χ) is referred to an absolute frame tied to the bottom of the simulation box. The ice film is schematically represented by the gray parallepiped.

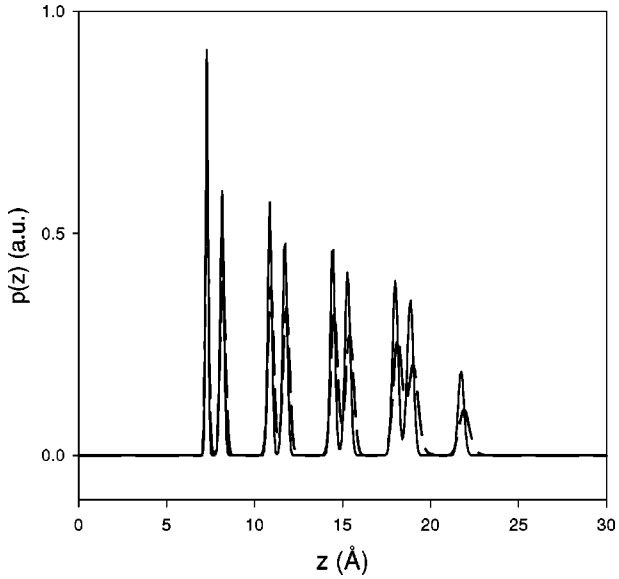

FIG. 2. Distribution function $p(z)$ (in arbitrary units, a.u.) of the distance z (Å) of the water and acetone molecular centers of mass from the bottom of the MD box, for an acetone coverage equal to 0.25. Full and broken curves correspond to $T=75$ and 150 K, respectively. Note that the two fixed water layers have not been represented.

water molecules. To simulate an infinite surface, periodic boundary conditions are imposed in the directions x and y parallel to the surface, by replicating the previous unit cell along (x,y) to give a rectangular MD simulation box of dimensions $x=35.92$ Å and $y=31.12$ Å . This box contains a total of 768 water molecules, 512 of them being moving molecules. The initial configuration of the water molecules[26] obeys the ice rules[13,14] and has no net charges or net dipoles.

The simulation box also contains a number of moving acetone molecules depending on the coverage considered. Here, we define the coverage as the number of acetone molecules adsorbed per number of water molecules in the surface layer, i.e., per bilayer of hexagonal ice. Based on the results obtained at 0 K from an optimization procedure of the ice/acetone potential,[21] the present calculations involve 32 acetone molecules per simulation box, which corresponds to a coverage of 0.25.

Each molecule is treated as a rigid rotor, and six external coordinates are used to describe the translation of the center of mass (x,y,z) and the orientation of the molecule (ϕ,θ,χ) with respect to an absolute frame tied to the bottom of the simulation box (Fig. 1) . The translational equations of motion are solved using the Verlet algorithm, and a predictor–corrector method based on the quaternion representation of the molecular orientations is used for the orientational equations,[27] with a time step of 2.2 fs. Every run involved an equilibration period ranging from 15 000 to 40 000 steps, depending on the temperature, followed by a production run of 15 000 or 20 000 steps. The configuration obtained by the optimization procedure at 0 K is used as the starting configuration. The initial linear and angular velocities for each moving molecule are taken from a Boltzmann distribution corresponding to the desired simulation temperature. This temperature is held constant during the production runs by scaling the velocities every ten steps. The cutoff in the calculations of the acetone–acetone, acetone–water, and water–water interactions is handled through three different neighbor lists,[27] with the same radial cutoff. Simulations are performed at 50, 75, 90, 100, 125, 140, and 150 K.

III. RESULTS

A. Structure and energy of the adlayer

Let us recall here briefly the results of the optimization procedure on the proton ordered ice surface at 0 K.[21] In this previous study, we have shown that the acetone molecules can wet the ice surface in order to form a perfectly ordered monolayer containing two acetone molecules per surface unit cell of ice. In this structure, corresponding to a coverage of 0.25 and referred as (1×1) phase, the molecular CO axes are nearly parallel to the ice surface, and they are mutually oriented in such a way that they form a herringbone structure $(\Delta\phi=|\phi_1-\phi_2|=60°)$. The centers of mass of the molecules are adsorbed at a distance $z=3.3$ Å from the midplane of the surface bilayer of water molecules, and this stable structure corresponds to an adsorption energy of -49 kJ/mol.

In the present simulations, we have investigated the structure of the acetone layer as a function of the temperature and for a coverage of 0.25, in order to study the stability of the monolayer found previously from the optimization procedure.[21] Preliminary tests were also performed in order to compare results obtained with larger simulation boxes. It is found that there are no significant differences in the simulations, whatever the temperature.

The distribution function $p(z)$ of the distances between the molecular centers of mass of the moving molecules and the origin of the absolute frame is shown in Fig. 2 at 75 and 150 K, and for a coverage equal to 0.25. The single peak around 21.5 Å corresponds to the acetone admolecules and it is a clear signature of the formation of one monolayer of acetone molecules above the ice crystal. This peak does not shift significantly when increasing the temperature (0.3 Å between 75 and 150 K), although it slightly broadens due to the thermal fluctuations. Note that, at these low temperatures,

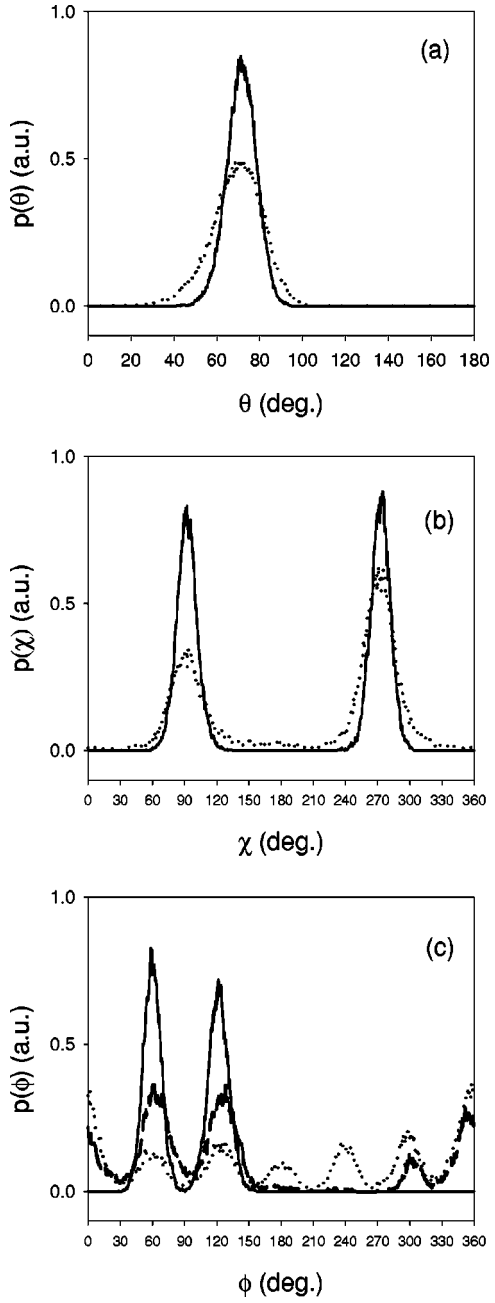

FIG. 3. Angular distribution functions for the acetone molecules at various temperatures (coverage 0.25): (a) θ angle; (b) χ angle; (c) ϕ angle. The angles are in degrees, and the distribution functions are given in arbitrary units (a.u.). Full and dotted curves correspond to $T=75$ and 150 K, respectively. The broken curve in (c) corresponds to an intermediate temperature, $T=125$ K.

the water bilayers exhibit vertical (z direction) translational ordering, as shown by the occurrence of double peaks in $p(z)$.

The angular distribution functions $p(\theta)$, $p(\phi)$, and $p(\chi)$ for the acetone monolayer are given in Fig. 3 at various temperatures. Note that we obtained the same distribution functions when starting the simulation with all acetone molecules standing upright (i.e., $\theta=0°$; this corresponds to CO bond perpendicular to the surface) instead of starting from the structure obtained from optimization, where all acetone molecules are flat on the surface. The distribution $p(\theta)$ always exhibits a single peak around 70° [Fig. 3(a)], the maximum position of which slightly depends on temperature (71.5°, 70.5°, and 69° at 75, 125, and 150 K, respectively) showing that acetone molecules are nearly flat on the surface. The angle less than 90° is mostly due to the steric volume of the methyl group. These values are about 10° lower than the equilibrium θ angle issued from the optimization at 0 K.[21] The full width at medium height (FWMH) of the $p(\theta)$ peak increases from 16° to 28° when temperature rises from 75 to 150 K. Note that this increase of FWMH becomes significant above 100 K, only. These features, connected to the asymmetry of the $p(\theta)$ peak toward the low angle values, indicate that the acetone molecules tend to lift up when the temperature increases. However, the behavior of $p(\theta)$ with temperature is typical of librational motions of the molecular axes around equilibrium. In the same way, the analysis of the distribution $p(\chi)$ [Fig. 3(b)] shows that the two methyl groups of the acetone molecule lie in the same plane parallel to the ice surface below 100 K, since $p(\chi)$ exhibits two equivalent peaks at 90° and 270°. This feature remains unchanged at higher temperature, but the peaks are broader, indicating that some methyl groups no longer belong to the plane parallel to the surface. By contrast, the function $p(\phi)$ [Fig. 3(c)] is characterized by a strong temperature-dependent behavior. Below 100 K, it exhibits only two peaks around 60° and 120°, which are close to the values obtained at 0 K[21] (59° and 122°). When the temperature increases, the $p(\phi)$ distribution tends to spread over the whole angular range, and new peaks are progressively evidenced (for example, around 0° at $T=125$ K).

These results show that on a proton ordered ice surface and below 100 K, acetone forms a perfectly ordered monolayer which contains two inequivalent molecules per water unit cell. These two molecules are slightly tilted (by about 20°) with respect to the ice surface plane, their CO axis pointing down to the surface and being mutually oriented in order to form an herringbone-like structure ($\Delta\phi=60°$). These features confirm the stability up to 100 K of the structure obtained in the optimization procedure, as illustrated in Fig. 4(a) by the snapshot issued from the simulation at 75 K. However, above this temperature a strong orientational disorder is evidenced in the angular distribution functions, especially for the ϕ angle, and the herringbone structure is no longer stable above 125 K. Moreover, the methyl groups which are on average close to a plane parallel to the ice surface at low temperature, tend to move away from the ice surface when the temperature increases [Fig. 4(b)].

The existence of the stable monolayer structure at low temperature is also evidenced by the analysis of various radial distribution functions $g(r)$. For example, the mutual arrangement of the centers of mass of the acetone molecules is given by $g_{\mathrm{CM-CM}}(r)$ [Fig. 5(a)], which represents the probability of finding two centers of mass a distance r apart. At small distances, this distribution does not change significantly with temperature, and it always exhibits a single peak at 5.96 Å . This peak corresponds to the distance between the first nearest acetone neighbors. At longer distances, $g_{\mathrm{CM-CM}}(r)$ exhibits two additional peaks below 100 K. They are much less structured at 125 K and vanish at higher

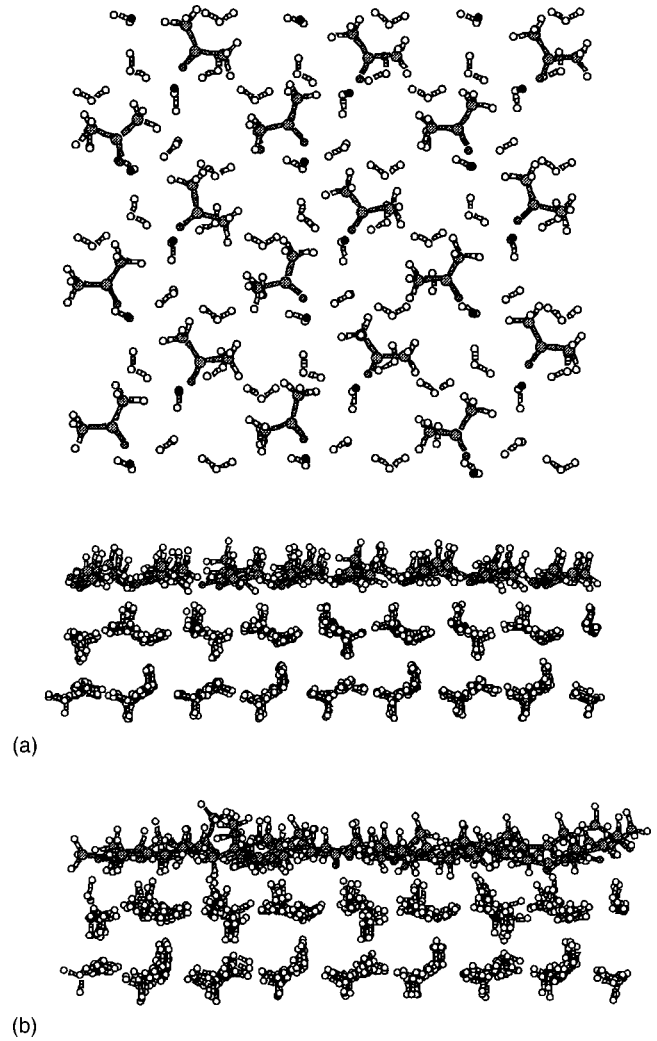

FIG. 4. Part of snapshots of the simulation with a coverage equal to 0.25: (a) top view and side view at 75 K, (b) side view at 150 K. The acetone molecules form an commensurate monolayer adsorbed above the ice film. Note the increasing mobility of the different molecules as the temperature increases. Only the top water layers are represented. On the top view, the dangling H atoms have been represented as black circles for clarity.

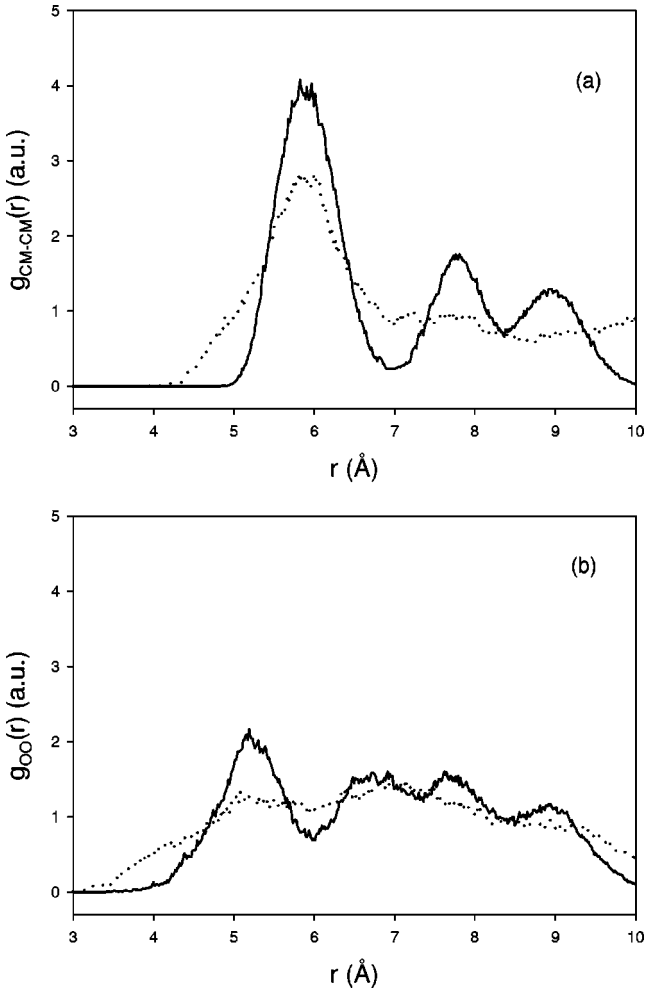

FIG. 5. Radial distribution functions $g_{CM-CM}(r)$ (a) and $g_{OO}(r)$ (b) for the acetone molecules at 75 (full curve) and 125 K (dotted curve). The distances are in Å , and the distribution functions in arbitrary units (a.u.). These results are issued from a simulation with a coverage equal to 0.25.

temperature, indicating that the long-range translational order is lost above this temperature. The integrated intensity of the first peak in $g_{CM-CM}(r)$ gives four molecules as nearest neighbors. This is in agreement with the occurrence of a (1×1) structure containing two acetone molecules per surface unit cell, related by two glide planes along the x and y directions. Note that no significant difference is observed for this three-dimensional (3D) distribution function $g(r)$ and the two-dimensional distribution function $g(r_{//})$ ($r_{//}$ being the projection on the surface plane of r, not given here), which is an additional proof for the planar structure of the acetone adlayer. The pair distribution $g_{OO}(r)$ [Fig. 5(b)] between the oxygen atoms of the acetone admolecules at different temperatures behaves similarly. Nevertheless, this latter distribution is much less structured than centers of mass distribution $g_{CM\text{-}CM}(r)$ at high temperatures and it mainly exhibits one first peak around 5.3 Å , which broadens as the temperature increases. At 150 K, the O atoms ordering is lost even at short range, while the centers of mass remain more or less ordered. This feature indicates that the lost in ordering is due primitively to orientational ϕ motions at higher temperature.

In order to investigate the tendency of acetone molecules to form bonds with the ice surface, we have plotted in Fig. 6(a) the 3D pair distribution $g_{O\text{-}Hw}(r)$ between an oxygen atom of the acetone molecules and a H atom of the underlying water molecules. This distribution mainly exhibits a strong peak centered at 1.81 Å , which does not significantly shift with temperature (less than 0.01 Å). Its integrated intensity, up to the first minimum, corresponds to the number of hydrogen atoms of water in the first shell around an oxygen atom of acetone. The present results correspond to one nearest-neighbor hydrogen atom of water per acetone oxygen. This feature, combined with an analysis of the snapshots issued from the simulation (see, for example, Fig. 4), indicates that each acetone molecule tends to form one hydrogen bond with a dangling OH of the ice surface (here, we define the hydrogen bond only on the basis of the O···H–O distance criterion), at investigated temperatures from 50 to 150 K. Moreover, the 2D pair distribution $g_{O\text{-}Hw}(r_{//})$ (where $r_{//}$ is the component parallel to the surface of the vector joining O

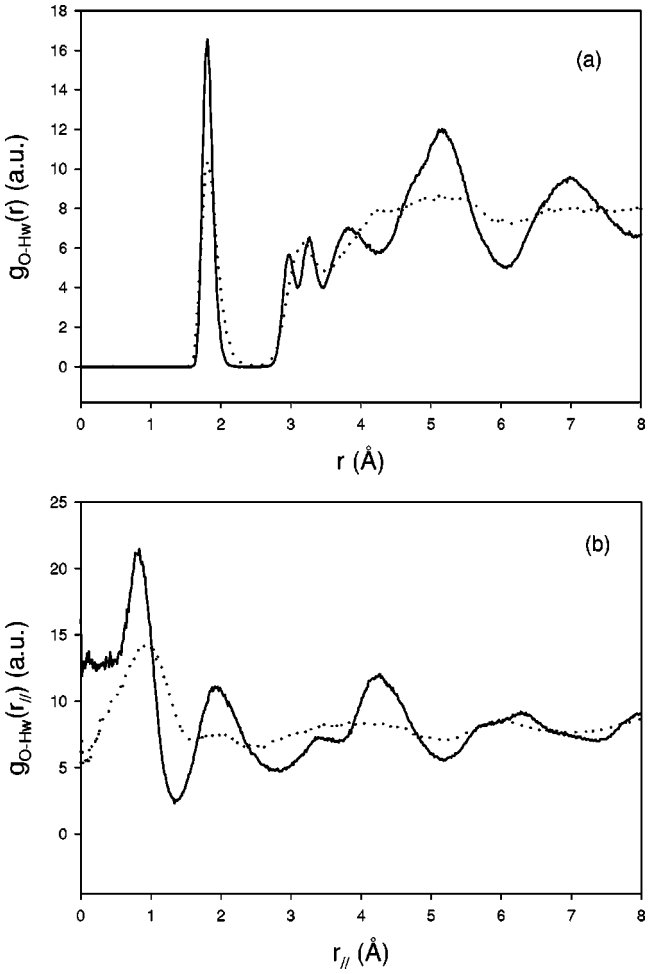

FIG. 6. Radial distribution functions $g_{\text{O-Hw}}(r)$ for the distances between the oxygen atom of the acetone molecule and the hydrogen atoms of water at 75 (full curves) and 150 K (dotted curves): (a) three dimensional distribution function, (b) two-dimensional distribution function (see the text). The distances are in Å , and the distribution functions in arbitrary units (a.u.). These results are issued from a simulation with a coverage equal to 0.25.

and Hw) is characterized by a first broad peak around 0.80 Å , indicating that the O atoms of the adsorbate are, in average, not adsorbed right above the OH dangling bonds which are perpendicular to the surface, but slightly displaced with respect to the H positions. Note that, at larger distances, $g_{\text{O-Hw}}(r)$ is more or less structured depending on the thermal fluctuations of the system.

The different contributions to the total energy of the system acetone–water are given in Table II. The acetone–acetone contribution V_{aa} slightly increases from 15% to 19% of the total potential energy when the temperature increases from 50 to 150 K, and it is mainly due to the dispersion–repulsion interactions. On the contrary, the acetone–water contribution is clearly of electrostatic nature, since V_{aw}^{E} represents about 80% of V_{aw} over the temperature range considered here. Note that the acetone–water contribution continuously decreases when the temperature increases due to the rearrangement of the acetone molecules which tend to lift up at high temperature. Taking into account the small contribution due to the kinetic energy, the total energy per acetone molecule ranges between -46.3 and -41.8 kJ/mol for the temperatures considered here.

B. Translational and orientational order

In the previous section, the examination of the translational and orientational distribution functions has shown that the structure of the acetone layer adsorbed on ice depends strongly on the temperature. In particular, the pair distribution functions $g(r)$ and the angular distribution $p(\phi)$ are strongly modified above 125 K, when the temperature increases. In order to discuss the reorientation and the loss of the ideal (1×1) structure of the acetone molecules, some translational and orientational order parameters have been calculated at different temperatures. Since the (1×1) herringbone-like structure is a superimposition of two sublattices, a translational order parameter is defined for each sublattice separately as

$$S_T(\mathbf{k}) = \frac{2}{N}\left\langle \left| \sum_j e^{i\mathbf{k}\cdot r_j} \right| \right\rangle, \tag{3}$$

where the summation accounts for molecules pertaining to one or the other sublattice. The symbol $\langle \cdots \rangle$ means that an average is performed over the duration of the simulation run and N is the total number of acetone molecules in the monolayer; $\mathbf{r}_j$ defines the position of the center of mass of molecule j in the absolute frame, and $\mathbf{k}$ is some reciprocal lattice vector. Not all $\mathbf{k}$ vectors can be investigated in the molecular dynamics simulation, as only those which conform to the periodic boundary conditions of the MD simulation box are accessible. In the present simulation, the patch is rectangular with sides parallel to the glide planes and contains 4×4 unit cells. Here, we are concerned only with $\mathbf{k}$ parallel to the surface, and we chose to investigate two $\mathbf{k}$ vectors, namely

TABLE II. Electrostatic and Lennard-Jones contributions (in kJ/mol) to the total energy per acetone molecule at monolayer coverage (i.e., 0.25) and for different temperatures.

Temp. (K)	V_{aa}^{E}	V_{aa}^{LJ}	V_{aa}	V_{aw}^{E}	V_{aw}^{LJ}	V_{aw}	V_{total}	Kin. energy	E_{total}
50	−0.32	−6.98	−7.3	−33.0	− 7.2	−40.2	−47.5	1.2	−46.3
75	−0.27	−6.89	−7.2	−32.3	− 7.2	−39.5	−46.7	1.8	−44.9
100	−0.22	−6.78	−7.0	−31.6	− 7.2	−38.8	−45.8	2.5	−43.3
125	−0.50	−6.70	−7.2	−30.5	− 7.1	−37.6	−44.8	3.1	−41.7
140	−1.50	−6.90	−8.4	−30.4	− 6.9	−37.3	−45.7	3.5	−42.2
150	−1.50	−7.00	−8.5	−30.0	− 7.0	−37.0	−45.5	3.7	−41.8

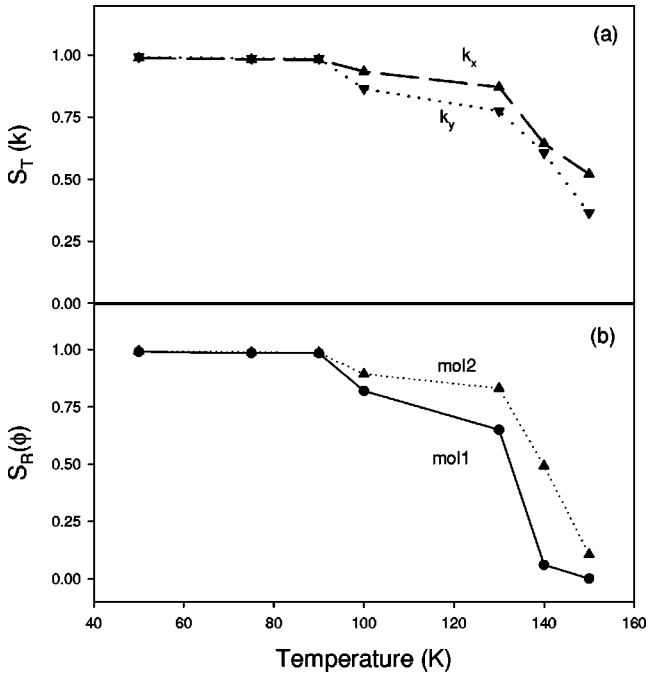

FIG. 7. (a) Translational order parameters along x and y directions as a function of temperature for one of the two sublattices of the herringbone structure formed by the acetone molecules (see the text). (b) Orientational order parameters (angle ϕ) for the two molecules in the unit cell of the acetone adlayer, as a function of temperature. These results are issued from a simulation with a coverage equal to 0.25.

$\mathbf{k}_x=(2\pi/a_x,0)$ and $\mathbf{k}_y=(0,2\pi/a_y)$ where a_x and a_y are the unit cell parameters of our ice lattice along the x and y directions, respectively.

Similarly, the orientational disorder for the CO molecular axis is monitored through the deviation from its ideal orientation Ω_e $[\Omega_e=(\phi_e,\theta_e)]$ in the (1×1) structure by calculating rotational order parameters for each sublattice, defined as

$$S_R(\Omega)=\frac{2}{N}\left\langle \sum_j \cos(\Omega_j-\Omega_e)\right\rangle, \tag{4}$$

where Ω stands for θ or ϕ.

For the perfectly ordered monolayer, the order parameter $S_{T,R}$ is equal to 1 for each sublattice, while it tends to zero for completely disordered structure. Figure 7(a) gives the translational order parameters for the two selected $\mathbf{k}$ directions, at different temperatures for one sublattice. The translational order parameter for the other sublattice is very similar. As can be seen from this figure, increasing the temperature leads to the disappearance of the ordered structure above 100 K, although some translational order remains in the adlayer since the order parameters do not vanish even at 150 K. These conclusions are consistent with the previous analysis of the $g(r)$ functions.

The calculated rotational order parameter $S_R(\phi)$ for the acetone adlayer is given in Fig. 7(b) for temperatures ranging between 50 and 150 K. The two angles θ and ϕ exhibit very different behavior as the temperature is increased. Indeed, $S_R(\theta)$ (not shown) remains nearly equal to 1, indicating that the molecular axes keep their tilt with respect to the surface plane, in the whole temperature range. On the contrary, ϕ disorder is evidenced above 100 K, and this angle exhibits a liquid-like behavior at 150 K. Again, these features are in agreement with the analysis of the angular distribution functions.

To summarize, the analysis of the order parameters and of various distribution functions demonstrates that, below 100 K, the acetone molecules can form a perfectly ordered commensurate monolayer on the proton ordered ice surface considered here. This monolayer has a (1×1) structure with respect to the ice unit cell since the acetone molecules are preferentially tied to the OH dangling bonds of the surface, and it contains two inequivalently adsorbed acetone molecules per unit cell. Above this temperature, this structure is no longer evidenced, although a certain translational order can persists at short range. The corresponding disordering is mainly due to the temperature dependence of the azimuthal angle ϕ, whereas the molecular axes remain tilted with respect to the ice surface over the whole range of temperature investigated here.

C. Preliminary results at lower and higher coverages

Although the present paper mainly focused on the structure of the acetone monolayer on proton ordered hexagonal ice, we have done some preliminary simulations by increasing the acetone coverage from 0.25 to 0.5 in order to investigate the completion of the monolayer. These simulations have been performed at two temperatures, namely 100 and 150 K. At temperature $T=100$ K, and with a coverage of 0.375, the analysis of the different distribution functions shows clearly that the acetone molecules form two layers: a first layer containing approximately 2/3 of the total amount of molecules, on which the remaining molecules tend to aggregate. This first layer is very similar to the monolayer obtained with a coverage of 0.25, for which each molecule is attached to an OH dangling bond, indicating that this coverage corresponds to the saturation of the ice surface. At higher coverage of 0.5 and T=100 K, the distribution function $p(z)$ of the z position of the centers of mass exhibits two peaks (located at 21.8 and 25.2 Å) which are of the same intensity. This indicates that the acetone molecules have arranged themselves in two layers above the ice surface containing the same number of molecules per layer, as illustrated in the snapshot of the corresponding simulation given in Fig. 8. The acetone molecules pertaining to the first layer are again tied to the OH dangling bonds of the ice surface, and the molecules in the two layers are adsorbed nearly parallel to the ice surface. These molecules tend to form dimers with antiparallel configuration from one layer to the other (as indicated by an arrow in Fig. 8), in order to optimize the lateral interaction.[24] At 150 K, this ordering is lost and the acetone molecules rather form a liquid-like layer above the ice surface.

The different contributions to the total energy for the acetone molecules in the bilayer are given in Table III, for two temperatures. In this bilayer, the acetone–acetone contribution V_{aa} is about three times greater than in the monolayer, indicating the large influence of the lateral interactions between the two acetone layers. The acetone–water contri-

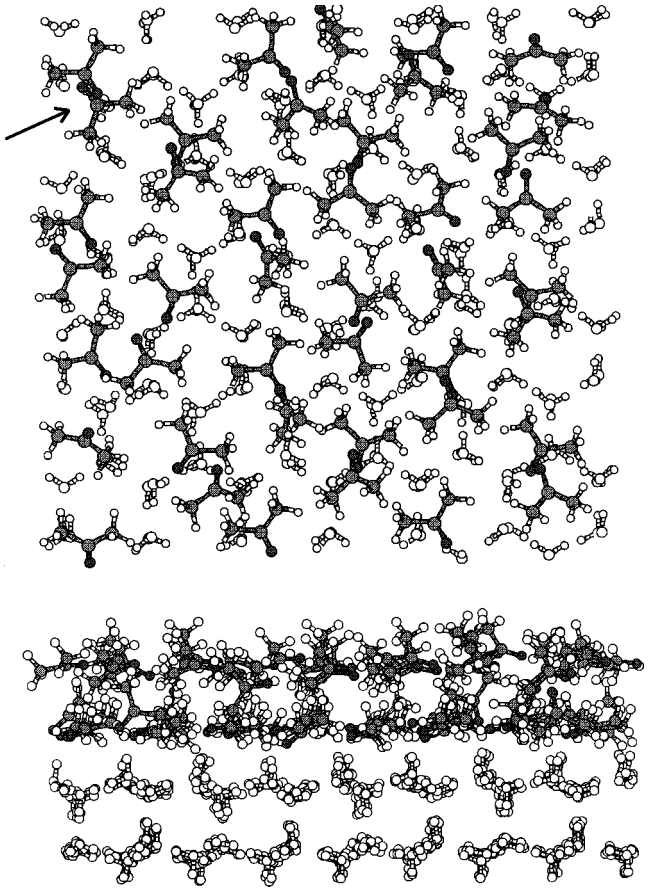

FIG. 8. Part of snapshots of the simulation with a coverage equal to 0.5: (a) top view and (b) side view at 100 K. The acetone molecules form two commensurate layers above the ice film. A characteristic antiparallel acetone dimer is indicated by the arrow (see the text). Only the top water layers are represented.

bution V_{aw} in the bilayer is nearly equal to V_{aa} since the interaction between the upper acetone layer and the ice crystal is very small (about 3 kJ/mol at 100 K). Taking into account the small contribution due to the kinetic energy, the total energy per acetone molecule ranges between -38.2 and -36.1 kJ/mol for the temperatures considered here (100 and 150 K). From these values, the estimation of the energy which would be necessary to desorb the acetone molecules pertaining to the upper layer ranges between -34.0 and -30.0 kJ/mol when the temperature increases from 100 to 150 K.

We have also done a simulation at 175 K by decreasing the coverage down to 0.125 on a large simulation patch containing 36 acetone molecules adsorbed above a slab of 1728 mobile water molecules (6 layers). The initial configuration was built by removing one half of the acetone molecules in the perfectly ordered (1×1) monolayer. A snapshot of the final configuration is given in Fig. 9, where two-dimensional clusters of acetone molecules are evidenced. On average, the admolecules are adsorbed nearly parallel to the ice surface and again, each admolecule is tied to an OH dangling bond of the ice surface. However, at this temperature, the acetone molecules are mobile enough to cluster on the ice surface. These aggregates can be viewed as precursor states for the completion of the monolayer. The corresponding contributions to the total energy are given in Table III.

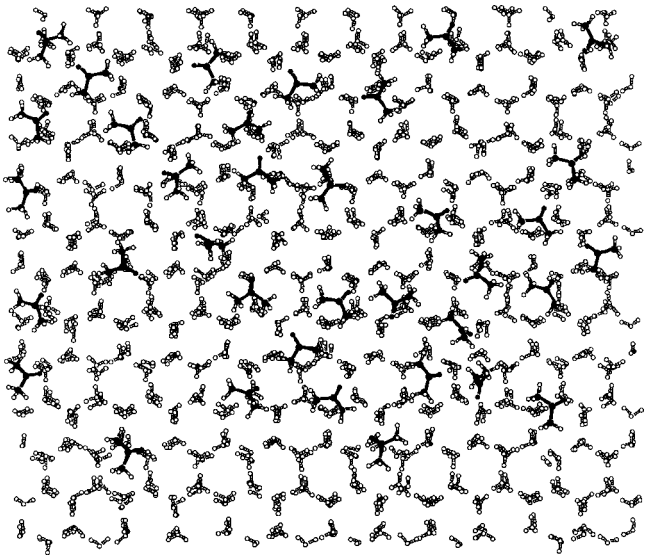

FIG. 9. Top view of a snapshot of the simulation with a coverage equal to 0.125. The acetone molecules, which are represented in black for clarity, tend to aggregate above the ice film.

IV. DISCUSSION

In this paper, molecular dynamics simulations based on classical potentials have been used to study the structuring of acetone molecules above a proton ordered hexagonal ice surface. The strong interactions between acetone molecules and water, responsible for the adsorption of these molecules on ice, in combination with the attractive lateral interactions between the admolecules, lead to the formation of a stable commensurate monolayer at low coverage (0.25). This monolayer exhibits a (1×1) structure with respect to the proton ordered ice surface considered here, with an unit cell containing two inequivalently adsorbed molecules. At tem-

TABLE III. Electrostatic and Lennard-Jones contributions (in kJ/mol) to the total energy per acetone molecule at submonolayer (i.e., 0.125) and bilayer coverages (i.e., 0.25) and for different temperatures.

Temp. (K)	V_{aa}^{E}	V_{aa}^{LJ}	V_{aa}	V_{aw}^{E}	V_{aw}^{LJ}	V_{aw}	V_{total}	Kin.energy	E_{total}
100[a]	−5.5	−15.1	−20.1	−16.1	− 4.5	−20.6	−40.7	2.5	−38.2
150[a]	−5.3	−14.9	−20.2	−15.1	− 4.6	−19.7	−39.8	3.7	−36.1
175[b]	−0.7	−3.5	−4.2	−31.8	− 7.2	−39.0	−43.2	4.3	−38.9

[a]Energies for the bilayer (coverage = 0.5).
[b]Energies at half monolayer coverage (0.125).

perature below 100 K, these two molecules are adsorbed nearly parallel to the ice surface plane, with their CO axes oriented in such a way to form a herringbone structure. These results, at finite temperature, confirm the stability of the structure found previously by optimization at 0 K.[21] When temperature increases above 100 K, our calculations show that this ordered (1×1) structure disappears, mainly due to thermal orientational motion. It is interesting to note that commensurate structure of polar molecules on ice has been recently observed in helium atom scattering experiments[28] where CHF_3 admolecules fill the periodic pattern of water rings in order to form a $p(1\times1)$ overlayer on the ice Ih(0001) surface, below 75 K.

It should be mentioned that the (1×1) structure we found depends closely on the number of OH dangling bonds present at the surface of the ice crystal considered in the calculations, since the simulations indicate that the oxygen atoms of acetone molecules are preferentially attached to these OH dangling bonds. In the present paper, the surface of the ice crystal we used exhibits a regular pattern of dangling OH bonds, and the perfect herringbone ordering of the acetone admolecules could be viewed as an artifact of the calculations. Based on the ice rules,[13,14] this crystal is by no means unique and other ice surfaces containing different numbers of OH dangling bonds can also be simulated. Anyway, the saturation of the hydrogen bonds by the acetone admolecules obtained in the present simulations is likely independent of the proton ordering. However, such simulations are not unreasonable since such ordered ice crystals are commonly used in quantum-mechanical studies.[29,30] Moreover, some proton order has been recently observed up to 150 K for ice films grown on Pt(111).[31,32]

The potential accuracy may modify slightly the orientation of the adsorbed molecules. However, the parameters used here were fitted to represent accurately the electric dipole moment of acetone, and to reproduce the configurations and energy of the water–acetone dimer when compared to *ab initio* calculations.[22] The transferability of these parameters to model the interaction with ice may be thus questionable; nevertheless, the adsorption energy that we found for the acetone molecules is consistent with recent experimental investigations[10,11] based on thermal desorption measurements (TPD) between 100 and 200 K. In these experiments, Schaff *et al.* have shown that acetone is molecularly adsorbed on the surface of annealed and unannealed ice deposited on W(100) or Pt(111), with an activation energy equal to 35 ± 2 kJ/mol on the annealed surface and to 39 ± 2 kJ/mol above the unnealed film of ice. These values are comparable to the present values of the adsorption energy for the monolayer (equal to -41.8 kJ/mol at 150 K). Note, however, that the calculations have been done on hexagonal ice while, in the experiments, the unannealed and the annealed films correspond rather to an amorphous phase and to the metastable cubic crystalline phase, respectively. In the calculations, we have also disregarded the presence of defects in ice.

The results of the present simulations compare fairly well with the experimental data available in the literature. Such a comparison is partial, since as far as we know, no experiment has been specifically devoted to the determination of the structure of the acetone layers adsorbed on the ice surface.

First, two types of adsorption sites have been evidenced on the amorphous film (α and β acetone species) in the TPD experiments,[10] while only the α species has been observed on the crystalline film, at least at high coverage. In fact, at lower coverage, the TPD spectra for the two ice films are rather similar, indicating that both acetone species are probably present at the surface. However, the signal associated with the β species rapidly saturates when the coverage increases on the crystalline ice surface, whereas it is still observed at higher coverage on the amorphous film.

It should be mentioned that the comparison of the coverages given in the experimental data with the coverage definition used in the present paper is not straightforward, since we do not refer to the same amount of molecules. Schaff *et al.*[10,11] defined 1 ML as the exposure necessary to form a saturated water or acetone adlayer on the underlying metal substrate, whereas we define the coverage as the ratio between the number of acetone molecules and the number of water molecules in our simulation box. Thus, preliminary theoretical study of the adsorption of water and acetone on the metal substrates used in the experiments (W and Pt) would be required to calculate coverages in the same way. Nevertheless, based on experimental study of the water adsorption on Pt(111),[33] which has shown commensurability between ice layers and the Pt surface, we might approximately estimate that the coverage of acetone on crystalline ice is the same as that on Pt(111). From this estimate, this means that our coverage is similar to the coverage given in the experimental papers.[10,11]

In the present study, we have found that, at monolayer coverage (i.e., 0.25) on the proton ordered surface of ice considered here, the unit cell of the adlayer contains two inequivalently adsorbed acetone molecules. These two molecules differ mainly by their azimuthal orientation and have almost the same adsorption energy. It is unlikely then that they correspond to the α and β species, which are separated in the TPD spectra by more than 20 K, thus indicating large adsorption energy difference. They would probably correspond rather to only one of the two species experimentally observed. When one compares the calculated adsorption energies (-41.8 kJ/mol at 150 K) with the measured desorption energies (-35 kJ/mol for α and -39 ± 2 kJ/mol for β-acetone species), it seems reasonable to assume that the present results correspond rather to the β species.

Moreover, besides TPD measurements, Fourier transform infrared experiments (FTIR) have also been conducted in order to investigate in detail the interaction between the carbonyl group of acetone and the OH dangling bonds of the ice films.[11] These FTIR experiments have shown that the β-acetone species is preferentially tied to an OH bond of ice, since the small IR peak corresponding to these dangling bonds disappears in the spectra upon acetone adsorption, even at low coverage, for both amorphous and crystalline ice. Furthermore, at very low acetone exposures and on both ice surfaces, the acetone CO stretch is shifted to lower frequency by about 14 cm^{-1}, which is consistent with hydrogen bond to the carbonyl oxygen. The intensity of this low fre-

quency peak saturates when the coverage increases, leading to growth of the IR peak at the bulk carbonyl frequency ($1717\ cm^{-1}$).

Such a preferential bonding between acetone and the OH dangling bonds of the ice surface is consistent with the result found here, since every acetone molecule in the monolayer is attached to a dangling hydrogen bond of the ice surface, with a distance O (acetone) $\cdots$ H (water) distance equal to 1.81 Å . The electrostatic contribution to the total adsorption energy is about 80%. Moreover, each acetone molecular plane (i.e. the plane containing the O and the three C atoms) is tilted by about 70° with respect to the *z* axis of the system, leading to bent configuration for the C–O$\cdots$H–O bond. The angle between the acetone molecular axis and the OH dangling bond is then equal to 110°, a value which is close to the most probable orientation of acetone with respect to the hydroxyl group (i.e., 120°) from a chemical point of view.[34] However, in our simulation, the O $\cdots$ H–O bond is not linear, since the O atoms of acetone are laterally displaced by 0.8 Å with respect to the H position. Such a configuration, which corresponds to a distorted hydrogen bond, comes from the dispersion forces which tend to optimize the coordination of the acetone molecules with the underlying water molecules. The resulting geometry of the acetone monolayer thus corresponds to a complete saturation of the hydrogen bonds at the ice interface and we can infer that the strong interaction with the ice surface is responsible for a shift of the IR peaks of the acetone molecules, especially for the CO stretch mode. Note that a careful theoretical analysis of the IR response of the acetone molecules in the monolayer, coupled with an experimental study using polarized infrared measurements, should be of great interest to confirm the nearly flat orientation of the acetone molecules.

In addition, preliminary simulations have been performed between 100 and 175 K by increasing the acetone coverage from 0.125 to 0.5. At low coverage (0.125) and high temperature (175 K), the acetone molecules are mobile enough to cluster above the ice surface, due to the influence of attractive lateral interactions. At T=100 K, and with a coverage of 0.375, the acetone molecules form a first complete monolayer on which the remaining molecules tend to aggregate. This monolayer is very similar to that obtained with a coverage of 0.25, indicating that this coverage corresponds to the saturation of the proton ordered ice surface. At higher coverage of 0.5 and T=100 K, the acetone molecules have arranged themselves in two layers above the ice surface containing the same number of molecules per layer. The desorption energy per molecule belonging to the upper layer ranges between -34 and -30 kJ/mol depending on the temperature, which is higher than the desorption energy of acetone molecules directly in contact with the ice surface. As a consequence, the desorption of a molecule pertaining to the upper layer is easier than the desorption of a molecule in the layer close to the ice surface. These values of the desorption energy for the upper adlayer are close to the experimental desorption energy for the α species (-35 kJ/mol).

Based on these results, it is tempting to identify the β species with the acetone molecules adsorbed directly above the ice surface and thus bound to the dangling hydrogen atoms, while the α species would rather correspond to acetone molecules pertaining to additional overlayers. Indeed, a crystalline surface of ice is certainly smoother than an amorphous surface, and exhibits much less OH dangling bonds.[35] Only few acetone exposures are thus necessary to saturate a crystalline surface of ice, to form a commensurate structure as indicated by the present simulations, whereas many more acetone molecules are required to saturate an amorphous surface of ice. Such an interpretation is consistent with the conclusions of Schaff *et al.*[10,11] regarding the ability of an amorphous ice surface to adsorb the acetone molecules when compared to a crystalline ice surface.

V. CONCLUSION

In this paper, we have presented a detailed simulation of the acetone adsorption on a crystalline ice surface, focusing mainly on structural properties at low coverage (i.e., one monolayer of acetone molecules). The analysis of dynamical information such as velocity autocorrelation functions and diffusion coefficients will be studied in a further work, together with a detailed study at higher coverage, especially in order to compare the ordering of the acetone overlayers with the acetone bulk structure. The present study on the adsorption of acetone on a crystalline surface of ice is in fair agreement with previous conclusions based on experimental data. A similar modeling of the acetone adsorption on proton disordered ice and on amorphous ice would certainly provide complementary results for a better understanding of the experiments.

[1] R. Zellner, *Global Aspects of Atmospheric Chemistry* (Springer, New York, 1999).
[2] B. J. Gertner and J. T. Hynes, Faraday Discuss. **110**, 301 (1998), and references therein.
[3] S. Solomon, Rev. Geophys. **26**, 131 (1988).
[4] C. Toubin, S. Picaud, and C. Girardet, Chem. Phys. **244**, 227 (1999).
[5] F. Arnold, G. Knop, and H. Zeiereis, Nature (London) **321**, 505 (1986).
[6] F. Arnold, V. Bürger, B. Droste-Fanke, F. Grimm, A. Krieger, J. Schneider, and T. Stilp, Geophys. Res. Lett. **24**, 3017 (1997).
[7] I. Folkins, R. Chatfield, H. Singh, Y. Chen, and B. Heikes, Geophys. Res. Lett. **25**, 1305 (1998).
[8] M. Kulmala, A. Laaksonen, P. Korhonen, T. Vesala, and T. Ahonen, J. Geophys. Res. **98**, 22949 (1993).
[9] L. Rey-Hanot, Thesis, Grenoble, 1999.
[10] J. E. Schaff and J. T. Roberts, J. Phys. Chem. **98**, 6900 (1994); **100**, 14151 (1996).
[11] J. E. Schaff and J. T. Roberts, Langmuir **14**, 1478 (1998).
[12] X. K. Zhang, E. G. Lewars, R. E. March, and J. M. Parnis, J. Phys. Chem. **97**, 4320 (1993).
[13] J. D. Bernal and R. H. Fowler, J. Chem. Phys. **1**, 515 (1933).
[14] D. Eisenberg and W. Kauzmann, *The Structure and Properties of Water* (Clarendon, Oxford, 1969).
[15] E. Cota and W. G. Hoover, J. Chem. Phys. **67**, 3839 (1977).
[16] J. A. Hayward and J. R. Reimers, J. Chem. Phys. **106**, 1518 (1997).
[17] V. Buch, P. Sandler, and J. Sadlej, J. Phys. Chem. **102**, 8641 (1998).
[18] W. L. Jorgensen, J. Chandrasekhar, J. F. Madura, R. W. Impey, and M. L. Klein, J. Chem. Phys. **79**, 926 (1983).
[19] H. Nada and Y. Furukawa, Surf. Sci. **446**, 1 (2000).
[20] M. J. Vlot, J. Huinink, and J. P. van der Eerden, J. Chem. Phys. **110**, 55 (1999).
[21] S. Picaud, C. Toubin, and C. Girardet, Surf. Sci. (in press).
[22] M. Ferrario, M. Haughney, I. R. McDonald, and M. L. Klein, J. Chem. Phys. **93**, 5156 (1990).
[23] J. C. Soetens, C. Millot, P. N. M. Hoang, and C. Girardet, Surf. Sci. **419**, 48 (1998).
[24] P. Jedlovszky and G. Palinkas, Mol. Phys. **84**, 217 (1995).

[25] K. Bolton, M. Svanberg, and J. B. C. Pettersson, J. Chem. Phys. **110**, 5380 (1999).
[26] V. Buch (private communication).
[27] M. P. Allen and D. J. Tildesley, *Computer Simulation of Liquids* (Clarendon, Oxford, 1987).
[28] A. P. Graham, A. Menzel, and J. P. Toennies, J. Chem. Phys. **111**, 1169 (1999).
[29] S. Casassa, P. Ugliengo, and C. Pisani, J. Chem. Phys. **106**, 8030 (1997).
[30] G. Bussolin, S. Casassa, C. Pisani, and P. Ugliengo, J. Chem. Phys. **108**, 9516 (1998).
[31] X. Su, L. Lianos, Y. R. Shen, and G. A. Somorjai, Phys. Rev. Lett. **80**, 1533 (1998).
[32] M. J. Iedema, M. J. Dresser, D. L. Doering, J. B. Rowland, W. P. Hess, A. A. Tsekouras, and J. P. Cowin, J. Phys. Chem. B **102**, 9203 (1998).
[33] J. Braun, A. Glebov, A. P. Graham, A. Menzel, and J. P. Toennies, Phys. Rev. Lett. **80**, 2638 (1998).
[34] A. Bródka and T. W. Zerda, J. Chem. Phys. **104**, 6319 (1996).
[35] V. Buch, L. Delzeit, C. Blackledge, and J. P. Devlin, J. Phys. Chem. **100**, 3732 (1996).